AD-A042 584 OFFICE OF NAVAL RESEARCH LONDON (ENGLAND) F/G 3/2
EFFICIENCIES OF VARIOUS METHODS FOR SOLAR ENERGY CONVERSION,(U)
JUN 77 W G SOPER
UNCLASSIFIED ONRL-R-6-77 NL

1 OF 1
ADA042584

END
DATE FILMED
8-77
DDC

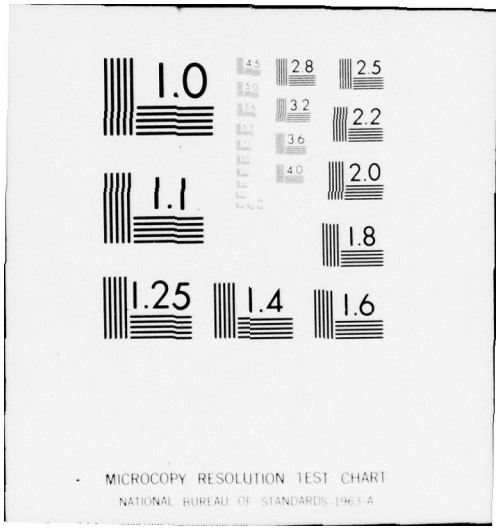
1.0
1.1
1.25
1.4
1.6
1.8
2.0
2.2
2.5
2.8
3.2
3.6
4.0
4.5
5.0
MICROCOPY RESOLUTION TEST CHART
NATIONAL BUREAU OF STANDARDS-1963-A

ONR LONDON REPORT

R-6-77

12

OFFICE OF NAVAL RESEARCH

BRANCH OFFICE LONDON ENGLAND

EFFICIENCIES OF VARIOUS METHODS FOR SOLAR ENERGY CONVERSION

W. G. SOPER

20 June 1977

UNITED STATES OF AMERICA

UNCLASSIFIED

SECURITY CLASSIFICATION OF THIS PAGE (When Data Entered)

REPORT DOCUMENTATION PAGE		READ INSTRUCTIONS BEFORE COMPLETING FORM
1. REPORT NUMBER ONRL-R-6-77	2. GOVT ACCESSION NO.	3. RECIPIENT'S CATALOG NUMBER
4. TITLE (and Subtitle) Efficiencies of Various Methods for Solar Energy Conversion		5. TYPE OF REPORT & PERIOD COVERED 6. PERFORMING ORG. REPORT NUMBER R-6-77
7. AUTHOR(s) W. G. SOPER		8. CONTRACT OR GRANT NUMBER(s)
9. PERFORMING ORGANIZATION NAME AND ADDRESS Office of Naval Research Branch Office, London, Box 39 FPO New York 09510		10. PROGRAM ELEMENT, PROJECT, TASK AREA & WORK UNIT NUMBERS
11. CONTROLLING OFFICE NAME AND ADDRESS		12. REPORT DATE 20 JUNE 1977 13. NUMBER OF PAGES 32
14. MONITORING AGENCY NAME & ADDRESS(if different from Controlling Office)		15. SECURITY CLASS. (of this report) UNCLASSIFIED 15a. DECLASSIFICATION/DOWNGRADING SCHEDULE

16. DISTRIBUTION STATEMENT (of this Report)

APPROVED FOR PUBLIC RELEASE; DISTRIBUTION UNLIMITED

17. DISTRIBUTION STATEMENT (of the abstract entered in Block 20, if different from Report)

18. SUPPLEMENTARY NOTES

19. KEY WORDS (Continue on reverse side if necessary and identify by block number)

Energy, solar energy, heat engines, water splitting, solar cells

20. ABSTRACT (Continue on reverse side if necessary and identify by block number)

Three methods are examined for converting solar energy to electricity or shaft work: heat engines, thermal decomposition of water to produce H_2, and solar cells. Maximum efficiencies of conversion are found to lie between 20% and 50%. For most applications, the heat engine is superior to the water splitting process.

DD FORM 1 JAN 73 1473 EDITION OF 1 NOV 65 IS OBSOLETE
S/N 0102-014-6601

UNCLASSIFIED
SECURITY CLASSIFICATION OF THIS PAGE (When Data Entered)

EFFICIENCIES OF VARIOUS METHODS FOR SOLAR ENERGY CONVERSION

by

W. G. SOPER

INTRODUCTION

Solar energy, essentially inexhaustible and non-polluting, is one of the alternative sources of power being investigated for future utilization. Methods for converting this electromagnetic radiation of 0.3-μm to 3.0-μm wavelength into more useful forms (electricity, shaft work, or chemical energy) are being proposed in great variety. It is the purpose of this report to examine some of these methods and to estimate their maximum efficiencies. From this information a partial assessment of the relative potential of the methods is made. As most of the material is not original, the report is principally a collection and condensation of ideas distributed through the technical literature. Apologies to specialist readers are made for simplifications necessary to keep the presentation straightforward and uncomplicated.

Methods for Solar Energy Conversion

The methods to be considered here are as follows:

1. Heat Engines

2. Decomposition of Water to Produce H_2

    a. Direct Thermal Splitting
    b. Two-Step Thermochemical Process
    c. Multi-Step Process

3. Solar Cells

    a. Photovoltaic
    b. Antenna-Type

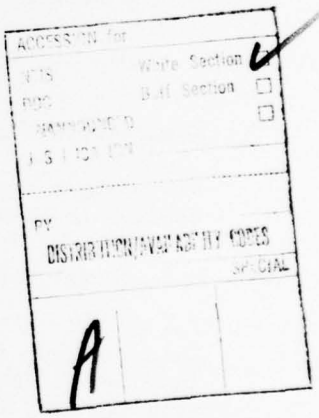

I. Heat Engines

This is the easiest method to assess in detail, because the technology of vapor cycles has been intensively developed over the past century. Maximum theoretical thermal efficiency (shaft work/heat input to cycle) is given by the familiar Carnot expression

$$\eta_C = (T-T_O)/T$$

where T is the temperature at which heat is fed into the cycle, and T_o that at which it is withdrawn. In terms of the equipment, T and T_o are temperatures of the boiler and condenser, respectively. To maximize performance we will take T_o to be the minimum temperature available--the ambient temperature.

To define the maximum boiler temperature that can be realistically achieved with solar radiation, we will use characteristics of a solar furnace. (This is clearly optimistic for a discussion of power production, as solar furnaces are designed to provide temperature, not power. Increase of heat transfer surface to improve power output will increase losses and reduce maximum temperature.) The maximum temperature attainable in a solar furnace is about 4000 K [1]. If energy loss from the boiler is assumed to be purely radiative and is taken to be proportional to the fourth power of boiler temperature, the heat available for the vapor cycle is the difference of the incident and radiated energies. This heat is given by

$$Q(T) = Q_o \left[1 - \left(\frac{T}{4000}\right)^4\right]$$

where Q_o is the solar energy incident upon the boiler. Efficiency of the boiler is defined by

$$\eta_B = Q(T)/Q_o = \left[1 - \left(\frac{T}{4000}\right)^4\right]$$

Losses in the reflector are not included in this accounting.

The maximum thermal efficiency of the overall system (boiler + engine) is given by the product of boiler and engine efficiencies:

$$\text{overall efficiency} = \eta_C \eta_B = \frac{T - T_o}{T}\left[1 - \left(\frac{T}{4000}\right)^4\right]$$

This quantity is the ratio of shaft work to the solar energy that impinges on the boiler, and it is plotted as curve 1 in Fig. 1 with T_o = 300 K. Peak efficiency is approximately 0.80, with an associated temperature of 1800 K (2780°F).

Remarks:

The preceding efficiency is an upper limit in two respects: Carnot efficiency is assumed for the engine, and solar furnace characteristics are assumed for the boiler. To bring engine performance closer to reality, we note that the efficiency of modern steam turbines (shaft work/heat input to steam) is

approximately 40% [2]. Maximum steam temperature is typically 1000°F or 810 K. Utilizing the quantity η_B for the efficiency of the solar boiler, we calculate the efficiency of (boiler + engine):

$$\text{overall efficiency} = 0.4 \times \left[1 - \left(\frac{810}{4000}\right)^4\right] \doteq 0.4$$

(Boiler efficiency is virtually unity for temperatures below 2000 K.) Thus, about 40% of the solar energy that impinges on the boiler is converted into shaft work. This performance, slightly greater than half the thermodynamic upper limit at 810 K, is indicated in Fig. 1 as a "more realistic estimate."

II. Thermal Decomposition (Splitting) of Water to Produce Hydrogen

This process differs fundamentally from that in (I.) in that fuel is manufactured; i.e., it is a conversion of solar to chemical energy. Of course, the H_2 will be eventually reacted with O_2 to provide either shaft power or electricity. In keeping with the objective of this analysis (to estimate maximum performance), this reaction will be assumed to have maximum theoretical efficiency. The free-energy content of the fuel upon reaction will be assumed to be converted completely into mechanical or electrical energy, and the efficiency will be computed as the ratio of this work to the heat required by the splitting process. This tacitly assumes use of an ideal fuel cell for conducting the reaction; combustion of H_2 in a heat engine is typically only 30% efficient [3].

a. Direct Thermal Splitting

Thermodynamic quantities ΔQ (heat required) and ΔF (work required) for the splitting of water are shown in Fig. 2. (More detailed data that include the ionization of H_2 and O_2 have been published [4], but use of these refined data would not alter the conclusion.) Free-energy change ΔF, the work required to split one mole of water within the prescribed mixture, is given by

$$\Delta F = RT \ln \frac{Q_p}{K_p(T)}$$

Here $K_p(T)$ is the equilibrium constant in terms of pressure [5], and Q_p is defined as

$$Q_p = P_{H_2} \times P_{O_2}^{\frac{1}{2}} / P_{H_2O}$$

where the P-terms denote partial pressures in atmospheres of the respective gases. The "standard" condition occurs when all partial

pressures are equal to 1 atm. This defines the free-energy change for the standard state,

$$\Delta F^{o} = -RT \ln K_p(T) ,$$

and from this one obtains

$$\Delta F = F^{o} + RT \ln Q_p$$

The preceding expression for ΔF is plotted in Fig. 2 for several combinations of partial pressures in the reacting mixture. From the abscissa-intercepts of the curves and from the previous remarks concerning the maximum temperature in a solar furnace, it is clear that, in mixtures where P_{H_2} and P_{O_2} are 1 atm or greater, it is not possible to split water without input of electrical work. It is necessary, then, either to provide electrical input of amount ΔF, or to operate with low partial pressures of H_2 and O_2 and thus reduce ΔF to zero at the temperature employed. In the latter case, however, work must be expended to compress the product gases to a useful level of pressure. To discard the O_2, for example, 1-atm pressure is required.

(In reality, work will also be required to separate the gases from the mixture, but here we assume ideal, selectively permeable membranes that permit separation of the gases with no pressure loss and no increase of entropy.)

To compute the compression work necessary to produce H_2 and O_2 at 1-atm pressure, we assume that the partial pressures P_{H_2} and P_{O_2} are reduced so that ΔF is substantially less than ΔF^{o} at temperature T. Then ΔF is given by

$$\Delta F(T) = \Delta F^{o}(T) + RT \ln Q_p ,$$

where $Q_p < 1$ and the last term is negative. Now the work per mole to compress the separated gases from pressure P_x back to 1 atm is

$$W_c = \int \frac{P\, dV}{n} = RT \ln \frac{1}{P_x} , \quad n = \text{number of moles.}$$

The total work to accomplish the splitting of water and production of gas at 1 atm is therefore (only ½ mole of O_2 is produced per mole of H_2)

$$W_T = \Delta F(T) + W_c = \Delta F(T) + RT \ln \frac{1}{P_{H_2}} + \tfrac{1}{2} RT \ln \frac{1}{P_{O_2}}$$

or

$$W_T = \Delta F^{o}(T) + RT \left[\ln \left(P_{H_2} P_{O_2}^{\frac{1}{2}}\right) - \ln \left(P_{H_2} P_{O_2}^{\frac{1}{2}}\right) \right] = \Delta F^{o}(T)$$

Thus, use of reduced gas pressures in the mixture just exchanges electrolytic work for compressor work; the total work required remains the same.

Having established that $\Delta F^{o}(T)$ can be employed in the analysis without loss of generality, we now compute the maximum thermal efficiency for a direct splitting process with a temperature of heat input T_u and eventual reaction of the H_2 at temperature T_o. For heat input Q at temperature T_u, the work input must be

$$W_I = \frac{Q\Delta F^{o}(T_u)}{\Delta Q^{o}(T_u)}$$

The quantity of H_2 produced will be

$$n_{H_2} = Q/\Delta Q^{o}(T_u)$$

If reacted reversibly to water at T_o, this H_2 will produce work equal to

$$W_H = n_{H_2}\Delta F^{o}(T_o) = \frac{Q\ \Delta F^{o}(T_o)}{\Delta Q^{o}(T_u)}$$

However, from this must be deducted the work required to perform the splitting at T_u, so the net work produced is

$$W_{net} = W_H - W_I = Q\left[\frac{\Delta F^{o}(T_o)}{\Delta Q^{o}(T_u)} - \frac{\Delta F^{o}(T_u)}{\Delta Q^{o}(T_u)}\right] = \frac{Q\ \left[\Delta F^{o}(T_o) - \Delta F^{o}(T_u)\right]}{\Delta Q^{o}(T_u)}$$

It is now assumed that (1) ΔH for the water decomposition reaction is not a function of temperature, and (2) the heat required to raise the incoming water at temperature T_o to the temperature of reaction T_u is exactly provided by the heat withdrawn in cooling the reaction products H_2 and O_2 back to T_o. Under these conditions, the $\Delta F^{o}(T)$ function must be a straight line (which, in fact, closely approximates the data for water), and the thermal efficiency of the splitting process assumes a familiar form:

$$\text{Efficiency of splitting} = \frac{W_{net}}{Q} = \frac{\Delta F^{o}(T_o) - \Delta F^{o}(T_u)}{\Delta Q^{o}(T_u)} = \frac{T_u - T_o}{T_u} = \eta_c$$

This is simply the Carnot expression; it relates the work potential of the H_2 product to the heat put into the splitting process. Now the ratio of this heat to the solar energy incident upon the process containment vessel, or "boiler," is the quantity

η_B. Thus the maximum overall thermal efficiency for a system that produces power by first splitting water with a solar furnace, and then reacting the H_2 reversibly, is the same as that for the heat engine: the product $\eta_c\eta_B$, or curve 1 of Fig. 1.

The general case where the heat capacities of the substances before and after reaction are not equal, and regenerative heating of the reactants by the products during cooling is not completely attainable, has been treated by Esteve *et al* [6], with the result that the efficiency of splitting is always less than the Carnot value η_c. The overall efficiency consequently falls below curve 1 of Fig. 1.

Remarks:

The preceding analysis has assumed that both the work output of the process and the work required for splitting can be provided with 100% efficiency by the reaction of H_2 at T_o. Only a fuel cell can approach this condition. Now a state-of-the-art fuel cell provides about 55% efficiency in converting H_2 free energy into electricity [7]. For this figure the thermal efficiency of the splitting process would be (retaining the ideal fuel cell for output power)

$$\frac{\Delta F^o(T_o) - (1/0.55)\ \Delta F^o(T_u)}{\Delta Q^o(T_u)}$$

This has been computed from the ΔF^o-data for water and combined with the solar boiler efficiency η_B. The result is plotted in Fig. 1 as curve 2. It is clear that the lower conversion efficiency has a drastic effect; temperatures above 2200 K are required to make the process self-sustaining. If a heat engine-generator were to provide power for splitting, its efficiency would be no better than 30%. This value gives curve 3 in Fig. 1. We conclude that solar power conversion through direct water splitting will be feasible only if very efficient means are available for (1) separating the gases from the mixture and (2) converting H_2 chemical energy into electrical work to assist the reaction, or into mechanical work to compress the gases. Nakamura [8] reaches similar conclusions in a much more detailed study.

b. Two-Step Splitting

The principal shortcoming of the direct process for water splitting is the need for input of work. Funk and Reinstrom showed in 1966 [9] that a properly chosen series of reactions can split water without the high temperatures or electrical work required by the direct process. The principle is illustrated in Fig. 3

with data from the ZnO process under study by the French solar furnace group at Odeillo [10]. The decomposition of water, reaction (3) in Fig. 3, is viewed as the result of two component reactions. In reaction (1), ZnO is decomposed endothermically ($\Delta H_1 > 0$) at T_u = 2200 K to yield Zn. In reaction (2), the Zn is combined with water exothermically ($\Delta H_2 < 0$) at T_ℓ = 1400 K to yield ZnO and H_2. At temperatures T_u and T_ℓ, the ΔF-values for reactions (1) and (2), respectively, are zero. Hence, no work is required to drive the reactions and accomplish the decomposition by this route.

The quantity of H_2 produced for heat input Q is

$$n_{H_2} = \frac{Q}{\Delta Q_1(T_u)} = \frac{Q}{\Delta H_1}$$

This H_2 will be cooled to ambient temperature T_o (heating the feed water to T_ℓ in the process) and eventually reacted with O_2 to produce work. The maximum work obtainable is (again assuming an ideal fuel cell)

$$W_{max} = n_{H_2}\ \Delta F3(T_o) = \frac{Q}{\Delta H_1}\ \Delta F3(T_o)$$

from which the thermal efficiency of splitting is W_{max}/Q, or $\Delta F_3(T_o)/\Delta H_1$. For the ZnO process in Fig. 3 the magnitude of this ratio is approximately 0.65; this value has been multiplied by the boiler efficiency η_B at 2200 K and entered in Fig. 1 as a theoretical maximum, point *.

The preceding was an actual case. The more general situation in two-step splitting is illustrated in Fig. 4 with the "straight-line" model. Here the thermal efficiency of splitting becomes

$$\eta_s = \frac{T_u - T_o}{T_u}\ \frac{\Delta F_3(T_o)}{\Delta F_1(T_o)}$$

We see that Carnot efficiency η_c can be attained by η_s, but only if $\Delta F_3(T_o)/\Delta F_1(T_o)$ is unity. This will in turn be true only if $T_\ell = T_o$; i.e., only if the exothermic reaction occurs at ambient temperature. In this case the overall efficiency (boiler + splitting process) is given by the product $\eta_c\eta_B$, or curve 1 in Fig. 1. If $T_\ell > T_o$, on the other hand, the ratio $\Delta F_3(T_o)/\Delta F_1(T_o)$ is less than unity, η_s is less than η_c, and the overall efficiency $\eta_s\eta_B$ falls below curve 1.

The geometry of Fig. 4 yields an alternative expression for η_s that points up the importance of the temperature difference $(T_u - T_\ell)$:

$$\eta_s = \frac{T_u - T_o}{T_u}\ \frac{\Delta F_3\ (T_o)}{\Delta F_1\ (T_o)} = \frac{T_u - T_\ell}{T_u}\ \frac{\Delta F_3(T_o)}{\Delta F_3(T_\ell)}$$

From this we see that the efficiency of splitting is basically that of a Carnot cycle based on T_u and T_ℓ, but enhanced by the fact that the H_2 is reacted at $T_o < T_\ell$.

c. Multi-Step Splitting

The slope of the $\Delta F_1(T)$ relationship in Fig. 4 is $(-\Delta S)$, as is clear from the thermodynamic expression

$$\Delta F = \Delta H - T\Delta S$$

in this ideal case where ΔH and ΔS are independent of T. As pointed out by Funk *et al* [9] and Bowman [11] and illustrated in Fig. 4, the slope must satisfy

$$\Delta S_1 = \frac{-\Delta F_3\ (T_\ell)}{T_u - T_\ell}$$

Now it is very difficult to find reactions whose entropy changes are great enough to keep $(T_u - T_\ell)$ conveniently small. Bowman gives ΔS = 76 cal/mole K (320 J/mole K) as a desired value based on T_u = 1100 K and T_ℓ = 400 K. Yet he points out that typical reactions provide only 25 cal/mole K. From this follows the widespread opinion that two-step processes will not be found suitable for water splitting. (The ZnO process described above provides a ΔS-value of approximately 45 cal/mole K; the resulting upper temperature T_u = 2200 K (3500°F) is beyond current industrial capability.)

The way out of this dilemma is to use more than two steps, as illustrated in Fig. 5. A series of reactions is chosen whose net $\Delta F(T)$ matches that of the previous endothermic reaction 1. The sum of the slopes satisfies

$$\left(\sum_{\text{endo.}} \Delta S\right) = \frac{-\Delta F_3(T_\ell)}{T_u - T_\ell}$$

Similarly, a set of exothermic reactions (not illustrated) is selected to match, in sum, the previous exothermic reaction 2. The resulting ΔS for all the reactions together must be

$$\left(\sum_{\text{endo.}} \Delta S\right) + \left(\sum_{\text{exo.}} \Delta S\right) = \frac{\Delta F_3(T_u) - \Delta F_3(T_\ell)}{T_u - T_\ell}$$

the entropy change for water decomposition.

The efficiency of the multi-step process can, under ideal conditions, equal that of the previously considered two-step process.

These conditions will exist if the crossing points ($\Delta F = 0$) of all the component endothermic reactions fall at a single temperature T_u, and those of all the component exothermic reactions at a single temperature T_ℓ. Otherwise, the efficiency (for specified maximum and minimum temperatures) will be less than that of the two-step process, because some of the heat will be transferred through less than the maximum temperature difference. (The example shown in Fig. 5 is a non-ideal case in this respect.)

From this brief discussion, we see that the maximum thermal efficiency of a system that splits water via solar heat and a multi-step process, then reversibly reacts the H_2 at ambient temperature to produce work, is the same as that of a solar-powered ideal heat engine that operates between the maximum temperature and ambient; i.e., the efficiency is described by curve 1 of Fig. 1. In any real process, however, there will be degradation factors associated with injection of heat at temperatures below the maximum and rejection of heat at temperatures above ambient.

Remarks:

About a dozen multi-step processes are currently being investigated, and Funk *et al* [12] have estimated efficiencies (realistic losses included) for several of them. These calculations are based upon the high heat value of H_2 at ambient temperature and not on the free energy; for use in this report an adjusting factor 0.8 has been applied. The resulting efficiencies lie in the range 0.2 to 0.4. Peak operating temperatures for the multi-step processes are about 1100 K. Utilizing the boiler efficiency η_B at this temperature, we estimate for a solar-powered splitting facility that

$$\text{Overall Efficiency} = (0.2 \text{ to } 0.4) \times \left[1 - \left(\frac{1100}{4000}\right)^4\right] \doteq 0.2 \text{ to } 0.4$$

These values have been plotted in Fig. 1 as "more realistic estimates."

In contrast to direct splitting, where the requirements for reversible internal processes are very severe, multi-stage splitting, according to Funk's results, appears feasible. No thermal splitting process has yet been implemented in an operating plant, however. Problems include the efficient recovery and reuse of auxiliary elements in the reactions, and the complexity of the physical plant when the process contains numerous steps.

III. Solar Cells

These are devices that convert the electromagnetic solar radiation directly into electricity, without first degrading it to

heat. They are accordingly not subject to thermodynamic limitations, there is no need for high temperatures, and there is no "boiler" heat loss. Still, there are factors that preclude complete conversion of solar to electrical energy.

a. Photovoltaic Cells

These cells function on quantum principles. To produce an electron-hole pair in the crystal, a minimum energy is required of the impinging quantum of radiation. Any excess of energy above this threshold level does not go into release of electrons, but is dissipated as heat. Now the energy of a quantum of radiation of wavelength λ is h/λ, h being Planck's constant. The fraction of radiant energy converted into electricity for a wavelength interval $d\lambda$ is therefore

$$\frac{\lambda}{\lambda^*} E_\lambda \, d\lambda \qquad (\lambda \leq \lambda^*)$$

where λ^* = wavelength associated with the threshold energy level
E_λ = energy per unit wavelength in the solar spectrum

The efficiency with which radiation releases electrical energy in the crystal can be expressed as

$$\int_0^{\lambda^*} \frac{\lambda}{\lambda^*} E_\lambda \, d\lambda \Big/ \int_0^{\lambda^*} E_\lambda \, d\lambda$$

Evaluation of these integrals with the appropriate expression [13] for E_λ

$$E_\lambda \left[\frac{W}{m^2\text{-}\mu m}\right] = \frac{3.66 \times 10^8 \, \lambda^{-5} \, [\mu m]}{e^{\frac{2.406}{\lambda \ \mu m}} - 1}$$

reveals that the efficiency attains a peak value of about 44% at $\lambda^* = 1.1$ μm, but exceeds 43% for 1.00 μm < λ^* <1.25 μm. The common silicon crystal has a λ^* of 1.15 μm; thus silicon is virtually optimized in regard to wavelength.

We see that an optimum photovoltaic device converts 44% of the sun's radiation into electricity. Unfortunately, however, all of this energy cannot be delivered to a load. A photovoltaic device can be represented by a generator and a resistor in series [14]. Elementary electrical theory (see Appendix 1) shows that such a circuit delivers maximum power to a load when the load resistance equals the device resistance. Under this condition, however, half the power developed by the generator is dissipated in the internal resistance of the device itself. Thus we arrive

at the often quoted result that the maximum efficiency of a photovoltaic device for converting incident radiation to electrical power is 22%. This level has been indicated in Fig. 1. Actual efficiencies as high as 18% have been claimed for some GaAs cells. Ten to twelve percent is typical of present Si cells, although 15% has been recently reported [15].

b. Antenna Cells

A second conceptual type of solar cell consists of an array of broad-band antennas for receiving the electromagnetic radiation and converting it into electricity. These are not quantum devices. They function by presenting to the incident electromagnetic wave an impedance that is approximately that of space. The waves accordingly enter the antenna with little reflection loss, and the weak alternating fields of the space waves are intensified by the geometry (for example, by the converging passage of a horn antenna) until detection and rectification of the signals are possible. There is at least one patent [16] covering an array of conical or tetrahedral elements (similar to the structure of the retina) designed for this purpose. A functioning device has not been built to date, however, because of the very small dimensions required of the antenna elements--approximately the wavelength of light.

With recent progress in fabrication of microcircuit components, there seems little doubt that such structures will eventually be made. For example, work on short-wavelength (x-ray) lasers at the U.S. Naval Research Laboratory, (Washington, D.C.) [17] shows promise of permitting the etching of microcircuits with dimensions much smaller than the wavelength of light. Furthermore, it is anticipated that wave interference patterns will be capable of producing the variation of intensity necessary for etching the fine detail of the microcircuits, eliminating the need for photo masks.

In the longer-wavelength IR region, Javan [18] and Schwarz [19] have already been successful in converting 10.6-μm radiation to electrical signals by means of tungsten wires etched to sharp conical tips. Schwarz is considering printed circuit arrays of such elements as improved IR detectors.

The advantage of a broad-band, antenna-type solar cell is that virtually all the incident radiant energy can be converted to electricity--at least in theory--as opposed to the limit of 44% in the conventional cell. Of course, the 50% loss due to internal heating at optimum load will still occur, so the maximum theoretical efficiency for converting solar radiation to electrical power will be 50%, vs 22% in the conventional cell. This is indicated in Fig. 1.

Discussion of Applications

This report has presented upper limits of performance for three classes of solar energy converters: heat engines, water splitting processes, and solar cells. It is fair to say that, in terms of efficiency, no process stands out as being clearly superior to the others. Thus, the ultimate value of any conversion method will depend upon (1) the cost and (2) any additional degradation factors that specific applications entail. This section examines various applications and discusses the factors that influence final output. Cost will not be addressed.

Because the element of cost is not considered, the discussion will be restricted to heat engines and water splitting processes. It is reasonable to expect that plants using heat engines and those using splitting processes might be comparable in cost. Thus, comparison of the plants' efficiencies alone will give a meaningful impression of their potential. This is not true for plants utilizing solar cells, where the technology is so different that initial and maintenance costs may be quite unlike those of the competitive methods. For solar cells, then, a comparison involving efficiencies alone would appear to be of little value.

The preceding sections have shown that heat engines and water splitting processes have (1) the same maximum theoretical efficiency and (2) similar efficiencies when real engines and real processes are considered. Thus, for the same maximum temperature, the shaft horsepower developed by a solar-driven steam turbine will be about the same as the free energy of H_2 produced by the splitting process. At this point in the comparison it becomes necessary to define the ultimate use of the energy. Four applications are discussed below.

a. Electrical Power Generation at the Solar Plant Site

In this application the turbine must be connected to an electrical generator, the efficiency of which will vary with size. Typical efficiencies are as follows [20]: 88% for 25 kW (equivalent to about 32 m^2 of incident sunshine), 96% for 3100 kW (1 acre of sunshine), and 99% for 70,000 kW (22 acres). For any plant of commercial significance, then, a generator efficiency of at least 95% should be attainable.

To generate electrical power from the splitting process, on the other hand, the H_2 produced must be either supplied to a fuel cell or used to fuel an internal-combustion engine/generator combination. Grüne *et al* [7] give the efficiency of a modern fuel cell to be 45% based on the high heating value of H_2, or about

55% based on free energy. We will adopt this figure in place of the idealization used in the preceding analysis of splitting; namely, that the free energy of the H_2 is converted into electricity by a perfect fuel cell with an efficiency of 100%. As discussed in Appendix 2, an H_2-fueled IC engine provides an efficiency of about 0.375 based upon free energy.

Combining the preceding data, we arrive at the following ratios of electrical power output P_E for plants using heat engines vs those using water splitting:

$$\frac{P_E \text{ (heat engine/generator)}}{P_E \text{ (splitting/fuel cell)}} = \frac{0.95}{0.55} = 1.73$$

$$\frac{P_E \text{ (heat engine/generator)}}{P_E \text{ (splitting/IC engine/generator)}} = \frac{0.95}{0.375(0.95)} = 2.67$$

Thus the fuel cell is substantially better than the IC engine/generator in utilizing the H_2 from the splitting process, and the heat engine is substantially better in producing power than either system that uses splitting.

b. Mechanical Power Generation at the Solar Plant Site

Here the shaft output of the heat engine can be used directly, while the splitting process must be combined with either a fuel cell and electric motor or with an IC engine. The appropriate ratios of mechanical power output P_M are as follows, where electric motor efficiency is taken to be 0.85 [21]:

$$\frac{P_M \text{ (heat engine)}}{P_M \text{ (splitting/fuel cell/motor)}} = \frac{1}{0.55(0.85)} = 2.14$$

$$\frac{P_M \text{ (heat engine)}}{P_M \text{ (splitting/IC engine)}} = \frac{1}{0.375} = 2.67$$

Here again, the heat engine is substantially better than the splitting process.

c. Production of H_2

In the future, H_2 may supplement electricity as an "energy vector" for transferring power from a central source, through a distribution network, to consumers [22]. To produce H_2 with a solar-powered heat engine, an electrical generator and electrolysis

unit would be used. The efficiency of electrolysis, based on free energy of the H_2 produced, will be taken to be 0.7 [22]. The relative output of the two conversion methods is given in terms of Q_H, the rate of H_2 production, by the ratio

$$\frac{Q_H \text{ (heat engine/generator/electrolysis)}}{Q_H \text{ (splitting)}} = 0.95(0.7) = 0.67$$

Here the splitting process, being more direct, has a definite advantage.

d. Vehicle Propulsion

Appendix 1 discusses batteries, and Appendix 2 compares vehicles powered by batteries with those powered by H_2 stored in hydride form. It is found that batteries are better from the standpoint of saving energy, since there is less loss in transferring the stored energy to the driving wheels. Hydrides, however, are better from the standpoint of weight. The hydride-powered vehicle outperforms the battery-powered vehicle of the same weight; therefore, for equal performance, the hydride-powered vehicle can be smaller and lighter.

(1) Comparison Using Electric and Hydride Vehicles

To compare solar power conversion by heat engine with that by splitting process, we first assume that the heat engine drives a generator to charge the batteries in an electric vehicle, while the splitting process replenishes the hydride in an H_2-powered vehicle. Electrical generator efficiency is taken to be 0.95, and losses in charging the batteries and in replenishing the hydride are assumed equal in magnitude and mutually canceling.

In this case, the results of Appendix 2, section B, pertain after the factor 0.95 is applied to the performance of the battery vehicle: the latter vehicle delivers about 35% more (payload x range) per unit solar energy than does a vehicle powered by an H_2-fueled internal-combustion (IC) engine, and about 10% more than a vehicle powered by a hydride/fuel cell/electric motor combination. In both cases, the battery-powered vehicle is substantially heavier than the H_2-powered machine.

(2) Comparison Using H_2-Powered Vehicles

In cases where the better payload/weight capabilities of the hydride vehicle would indicate its use, it is clear that the splitting facility will outperform the heat-engine plant. From

the previous discussion under "Production of H_2," we conclude that the heat-engine plant will produce only 67% as much H_2 fuel as the splitting facility.

Conclusions

Conclusions relative to conversion methods are as follows:

1. All methods proposed for converting solar energy to electrical, mechanical, or chemical energy have inherent shortcomings that reduce efficiency. Realistic expectations for maximum efficiency might be 40% for heat engines and multi-step water splitting processes, and 20% for photovoltaic solar cells. Antenna-type solar cells, which hold promise of higher efficiencies than photovoltaic cells, deserve further basic research and development.

2. Direct water splitting requires a combination of high temperatures and highly reversible internal processes that seems unlikely to be achieved in a viable commercial operation.

3. The heat engine is superior to the multi-step splitting process in the following applications, by the factor noted:

- mechanical power generation: 2.1
- electrical power generation: 1.7
- vehicle propulsion
  - battery vehicle vs H_2 vehicle with IC engine: 1.4
  - battery vehicle vs H_2 vehicle with fuel cell/electric motor: 1.1

4. The multi-step splitting process is superior to the heat engine in the production of H_2, by the factor 1.5.

Conclusions relevant to vehicle propulsion techniques are as follows:

1. For (a) state-of-the-art batteries and hydrides, and (b) vehicle performance rated in terms of (payload x range)/(energy stored), the battery vehicle outperforms the H_2 vehicle with IC engine by about 40%, and the H_2 vehicle with fuel cell and electric motor by 15%. The weight of the battery vehicle is approximately twice that of the H_2 vehicle.

2. For vehicle performance rated in terms of (payload x range)/(vehicle total weight), the H_2 vehicle outperforms the battery vehicle by about 2:1.

References

1. A. M. Zerem and D. D. Erway, *Introduction to the Utilization of Solar Energy* (McGraw-Hill Book Co., Inc., New York, 1963), Chap. 6.

2. L. S. Marks, *Mechanical Engineers' Handbook* (McGraw-Hill Book Co., Inc., New York, 1951) 5th ed., chapter on steam turbines, p. 1147-1172.

3. R. L. Wooley and G. J. Germane, "Dynamic Tests of Hydrogen-Powered IC Engines," First World Conference on Hydrogen Energy, Miami, Florida, Feb. 1976.

4. S. Ihara, "Feasibility of Hydrogen Production by Direct Water Splitting at High Temperature," ibid.

5. S. Glasstone, *The Elements of Physical Chemistry* (D. Van Nostrand Co., New York, 1957), Chapter X.

6. B. Esteve and J. P. Roncato, "Thermodynamique des Cycles Thermichimiques de Decomposition de l'Eau," International Conference on Hydrogen and Its Prospects, Liège, Belgium, Nov. 1976.

7. H. Grüne, H. B. Butbier, and K. Strasser, "H_2/O_2 Fuel Cell Assemblies with Higher Power Densities," Tenth International Power Sources Symposium, Brighton, England, 13-16 Sept. 1976.

8. T. Nakamura, "An Investigation of Hydrogen Production from Water at High Temperatures," Miami Conference.

9. J. E. Funk and R. M. Reinstrom, "Energy Requirements in the Production of Hydrogen from Water," *I&EC Process Design and Development*, Vol. 5, July 1966.

10. H. Herman, "Solar Furnaces in the Pyrenees," *ESN*-30-7, p. 315, July 1976.

11. M. G. Bowman, "Chemistry of Thermochemical Cycles from USA Programs," Liège Conference.

12. J. E. Funk and K. F. Knoche, "Thermochemical Hydrogen Production: Engineering Efficiency and Economics," Liège Conference.

13. A. I. Brown and S. M. Marco, *Introduction to Heat Transfer* (McGraw-Hill Book Co., Inc., New York, 1958), p. 51.

14. Reference 1, Chapter 8.

15. Monthly Activity Report, ONR Chicago Branch Office, Feb. 1977; report of presentation by H. Brandhorst (NASA/Lewis) to 1977 Annual Meeting of American Physical Society, Chicago, 7-11 Feb. 1977.

16. R. L. Bailey, "Electromagnetic Wave Energy Converter," NASA Patent Case GSC-11394-1, filed 27 Sept. 1972.

17. *NRL R&D Highlights*, March 1977, "Short-Wavelength Laser-Radiation Development."

18. A. Javan, "Laser Measures Light-Wave Frequency," *IEEE Spectrum* 8, 91, (Oct. 1971).

19. Monthly Activity Report, ONR Pasadena Branch Office, Feb. 1977; report of work in IR antennas by Professor S. Schwarz at UC/Berkeley.

20. Reference 2, p. 15-57.

21. Ibid, p. 15-65.

22. W. G. Soper, "International Conference on Hydrogen and Its Prospects," Report No. ONRL-C-40-76, ONR Branch Office, London, 31 Dec. 1976.

23. J. Birge, J. T. Brown, W. Feduska, C. C. Hardman, W. Pollack, R. Rosey, and J. Seidel, "Performance Characteristics of a New Iron-Nickel Cell and Battery for Electric Vehicles," Brighton Conference.

Also,

W. G. Soper, "The Tenth International Power Sources Symposium" Report No. ONRL-C-30-76, ONR Branch Office, London, 21 Oct. 1976.

24. O. von Krusenstierna, "High-Energy Long-Life Zinc Battery for Electric Vehicles," Brighton Conference.

25. W. J. Walsh and H. Shimotake, "Performance Characteristics of Lithium-Aluminum/Iron Sulfide Cells," Brighton Conference.

26. A. Gibson, "A Study of the Electrode Interface Formed between Sodium Metal and Beta Alumina Solid Electrode," Brighton Conference.

27. R. Schmitt, "Technische und Wirtschaftliche Aspekte der Wasserstoff-Speicherung in Metallhydriden," Liège Conference.

APPENDIX 1: Characteristics of Batteries

The performance of a battery is illustrated by the simple model in Fig. A1. The battery is represented by a voltage source V in series with a resistor r that simulates the resistance of the various internal elements to flow of current i. The load is represented by a resistor R. Power delivered to the load is given by

$$P = i^2R = \left(\frac{V}{R + r}\right)^2 R = \frac{V^2}{r} \frac{R/r}{(1 + R/r)^2}$$

Maximum power P_m is delivered when $R/r = 1$, so

$$P_m = \frac{1}{4} \frac{V^2}{R}$$

and

$$P = 4P_m \frac{R/r}{(1 + R/r)^2}$$

The energy U delivered to the load is expressed in terms of the total energy U_m stored in the battery by

$$\frac{U}{U_m} = \frac{i^2R}{i^2(R + r)} = \frac{R/r}{1 + R/r}$$

In Fig. A2 is plotted P/P_m vs U/U_m for various values of R/r. Maximum energy is delivered to the load when the load resistance is very high and the power delivered is very low. As load resistance is decreased, power delivered increases, but the energy delivered decreases, because of the resistive loss i^2r within the battery. Peak power is delivered when R = r; here exactly half the energy is delivered to the load while the other half is dissipated as heat within the battery. Values of $R/r < 1$ represent wasteful load settings that would be avoided in practice.

Fig. A3 presents power-energy data for several promising types of batteries. Power and energy "densities" are employed; i.e., the qualities are expressed per unit of battery mass. The Ni-Fe (Edison) and Ni-Zn cells described in the figure are essentially ready for production, having been road tested in electric vehicles. The other two types are high-temperature cells and are still in the experimental category. The familiar lead-acid battery, not shown, has a maximum energy density of about 25 Wh/kg.

APPENDIX 2: Vehicle Performance as Determined by Energy Storage Characteristics

Speed and range of vehicles powered by batteries or other chemical storage systems are controlled by the quantity of energy stored and the rate at which it can be withdrawn. These factors are in turn fixed by the fraction of vehicle weight allocated to storage and by the energy density and power density of the storage medium.

I. Power Requirements

To obtain an estimate of the power required by a typical vehicle, we note that the average thrust required to propel a rubber-tired vehicle under "town" conditions is about 1/16 of the vehicle weight [24]. This constant thrust provides a usable approximation up to perhaps 40 mph, where air drag is no longer small. (The fractions for light suburban driving and severe stop-and-go driving are 1/25 and 1/10, respectively.) Thus, range R and speed S are given in terms of energy density ε and power density ϕ by

$$R = 16\ \eta\ \frac{E}{T}\ \frac{\varepsilon}{g}$$

$$S = 16\ \eta\ \frac{E}{T}\ \frac{\phi}{g}$$

Here E and T are the weights of the energy storage medium and the total vehicle, respectively, η is the efficiency with which energy is converted from the storage medium to the driving wheels of the vehicle, and g is the acceleration of gravity. (Loss of energy through internal resistance of the battery is included in the battery $\phi(\varepsilon)$ function and is not part of η.)

For ε and ϕ in units of Wh/kg and kW/kg, the quantities R and S in units of miles and mph are given by

$$R[\text{miles}] = 3.65\eta\ \frac{E}{T}\ \varepsilon\ \left[\frac{\text{Wh}}{\text{kg}}\right]$$

$$S[\text{mph}] = 3.65\eta\ \frac{E}{T}\ \phi\ \left[\frac{\text{kW}}{\text{kg}}\right]$$

For battery-powered vehicles we take $\eta = 0.85$ to represent the efficiency of the electric-drive motor and obtain

$$R = 3.10\ \frac{E}{T}\ \varepsilon \qquad S = 3.10\ \frac{E}{T}\ \phi \qquad \ldots\ (1A)$$

In vehicles powered by IC engines operating on H_2 (stored, for example, in hydride form), only about 30% of the high heating value of H_2, or 37.5% of the free energy, is converted to shaft horsepower [3]. Thus η will be taken to be 0.375 for these systems, and the corresponding expressions for range and speed become

$$R = 1.37 \frac{E}{T} \varepsilon \qquad S = 1.37 \frac{E}{T} \phi \qquad \ldots \text{(2A)}$$

II. Comparison of Battery-Powered and H_2-Powered Vehicles

As shown in Appendix 1, energy density for batteries ranges from 45 Wh/kg for good state-of-the-art batteries to about 200 Wh/kg for advanced high-temperature cells. On the other hand, energy density for hydrides (converted to free energy) ranges from 240 Wh/kg for the readily decomposed compound $FeTiH_2$ to 3200 Wh/kg for LiH, which has a high heat of dissociation (25 kWh/kg H_2) and an equilibrium temperature of 800°C [27]. We will select 50 Wh/kg and 240 Wh/kg to represent batteries and hydrides, respectively, recognizing that substantial improvements can be made in both.

a. Fixed Vehicle Weight

A comparison between battery (B) and hydride (H) vehicles of the same total weight will be based upon the following expression, derived from equations 1A and 2A:

$$\frac{R_B}{R_H} = \frac{3.10}{1.37} \left(\frac{E}{T}\right)_B \left(\frac{T}{E}\right)_H \frac{50}{240} = 0.471 \left(\frac{E}{T}\right)_B \left(\frac{T}{E}\right)_H$$

or

$$\frac{R_B}{R_H} = 0.471 \frac{E_B}{E_H}, \quad \text{since } T_B = T_H . \qquad \ldots \text{(3A)}$$

It will be assumed that E = T/3 for the battery vehicle (BV). This value, which is typical of current designs, probably represents a practical upper limit for a machine that must have a substantial frame and body and must carry a useful load. Further, the payload L of the BV will be taken to be T/3, leaving a frame weight of T/3.

The ratio E/T in the hydride vehicle (HV) will be assumed to have a maximum value of 1/3, but may in general be smaller. The frame weight will be set at T/3, and the payload will be $L_H = T_H - E_H - (1/3)\ T_H$.

Substituting the assumed weight ratios into equation 3A, we obtain

$$\frac{R_B}{R_H} = 0.471 \left(\frac{1}{3}\right)\left(\frac{T}{E}\right)_H$$

or

$$\frac{R_B}{R_H} = \frac{0.471}{2-3\left(\frac{L}{T}\right)_H}$$

From this expression the following conclusions are drawn: If the payload of the HV is made equal to that of the BV ($L/T = 1/3$), then $R_H/R_B = 1/0.471$, and the range of the HV is 2.1 times that of the BV. If the ranges of the two vehicles are made the same, then $(L/T)_H = 0.510$ (as opposed to the value 1/3 assumed for the BV), and the HV carries a payload 53% larger than that of the BV.

In every case, however, the HV consumes more stored energy per mile than does the BV, because of the less efficient IC engine. The superiority in range and payload arises from the higher energy density of the storage medium; the HV simply carries more energy with it.

b. Fixed Stored Energy

A better comparison of the two vehicles, which takes account of the difference in efficiencies, will be based upon a quantity M, the product of payload and range for a given quantity of energy stored in the vehicle. Thus the ratio of energies stored in the vehicles is

$$\frac{\text{energy (battery)}}{\text{energy (hydride)}} = \frac{E_B\,\varepsilon_B}{E_H\,\varepsilon_H} = 1$$

From equations 1A and 2A, the ratio of terms R' (the range per unit of stored energy) is

$$\frac{R'_B}{R'_H} = \frac{3.10}{1.37}\,\frac{T_H}{T_B}$$

If L_B is again taken equal to $T_B/3$, the ratio of payloads is

$$\frac{L_B}{L_H} = \frac{1}{3}\,\frac{T_B}{L_H}$$

Finally, the ratio of the quantities M is

$$\frac{M_B}{M_H} = \frac{L_B}{L_H}\,\frac{R'_B}{R'_H} = \frac{3.10}{1.37}\,\frac{T_H}{T_B}\,\frac{1}{3}\,\frac{T_B}{L_H} = \frac{0.754}{L_H/T_H} \qquad \ldots \text{(4A)}$$

Since $L_H/T_H = 2/3 - E_H/T_H$, the range of L_H/T_H is from 1/3 to 2/3, corresponding to the range of E_H/T_H from 1/3 to zero. (Since the quantity of energy stored in the vehicle is by assumption constant, E_H is constant, and E_H/T_H can change only by variation of T_H.)

Equation 4A yields the result that M_B/M_H varies from 2.26 for $L_H/T_H = 1/3$, to 1.13 for $L_H/T_H = 2/3$. Thus the BV outperforms the HV for all possible values of E_H/T_H. The parameters are displayed in Fig. A4 for the full range of E_H/T_H. We note that when payloads are equal ($L_B/L_H = 1$), the BV has greater range than the HV, and when ranges are equal ($R'_B/R'_H = 1$) the BV has a greater payload. At $E_H/T_H = 0.14$, a reasonable point at which to compare the two vehicles, the value of M is 1.43.

While the BV is more energy-efficient, it is, however, heavier than the HV. The ratio of total weights is

$$\frac{T_B}{T_H} = \frac{T_B}{E_B}\,\frac{E_B}{E_H}\,\frac{E_H}{T_H} = 3(4.56)\,\frac{E_H}{T_H}$$

This is plotted in Fig. A4, and we see that the BV weighs about twice as much as the HV when ranges and payloads are comparable. Thus, although the BV delivers more ton-miles per unit stored energy, the vehicle itself will probably cost substantially more than the HV. If vehicle cost were included in the criterion of performance, the relative standing of the vehicles might be changed.

The performance of the two vehicles depends, of course, upon the efficiencies assumed for the propulsion systems. An IC engine has been assumed for the HV because of its simplicity. If, however, a fuel cell/electric motor combination were employed, a reasonable value for the efficiency η would be 0.85 x 0.55 = 0.47, and the range equation 2A would become

$$R = 1.71\,\frac{E}{T}\,\varepsilon$$

In this case, only the expressions for range and M change, as follows:

$$\frac{R'_B}{R'_H} = \frac{3.10}{1.71}\frac{T_H}{T_B} = 1.81\,\frac{T_H}{T_B}$$

$$\frac{M_B}{M_H} = \frac{3.10}{1.71}\frac{T_H}{L_H} = \frac{0.604}{L_H/T_H}$$

The functions are plotted in Fig. A4 as dotted lines. Here the BV is inferior to the HV for small E_H/T_H, but shows about 15% superiority when payloads and ranges of the two vehicles are comparable. Again, though, the BV is heavier than the HV, by about 70%. (It is noted in passing that no allowance was made in the HV for fuel burned to provide heat to the hydride, a function conveniently accomplished with the exhaust heat of an IC engine.)

This comparison has not included the speeds of H_2- and battery-powered vehicles, because we do not have appropriate ϕ-ε data for hydrides. Power will be determined by the rate of H_2 release from the hydride, and this release will require input of heat to maintain temperature and provide the heat of dissociation. Thus the power available will depend upon the characteristics of the heat exchanger. Schmitt [27] has published useful data relating the H_2 release rate to temperature and pressure for several hydrides.

There is a parallel in batteries to the heat requirements of a hydride system. It has been tacitly assumed in Appendix 1 that the heat dissipated within the battery at high power settings is promptly removed, so that battery temperature remains constant. If this is not the case, power output will be restricted, and the power-energy plots shown in Fig. A3 will not be achievable. Thus, heat transfer considerations must be included in the design of both hydride and battery systems, but in batteries heat must be removed from the storage medium.

III. Estimates of Range and Speed

In the preceding comparisons between battery and hydride systems, absolute ranges were not computed. A quick estimate of range and speed capabilities for given battery (or hydride, if $\phi(\varepsilon)$ is known) characteristics can be made as follows from equations 1A and 2A: To maximize the range performance of the vehicle we will take $E/T = 1/3$. Then equation 1A indicates that, in a BV, the range and speed will be given approximately by the numerical magnitudes of ε and ϕ of the battery. Referring to Fig. A3, for example, we see that this first-generation BV would have a maximum range of about 55 miles with the Ni-Zn battery.

This could be achieved, of course, only by proceeding at very low speed. On the other hand, the graph of $\phi(\varepsilon)$ indicates that the vehicle could make 35 mph for over 45 miles before exhausting the battery.

This simple model requires modification to be quantitatively useful at high speeds, where air resistance will alter the assumed condition of constant thrust. Another complication is the fact that resistance to motion, as defined in reference 24 for different driving conditions and used in this model, includes a certain amount of braking action. Thus the figure for "town" driving, for example, is based upon an (unspecified) average speed and frequency of stops, and to apply it to a range of speeds--as was done in the preceding paragraph--is inconsistent. The remedy, of course, is a model that includes separately the rolling resistance, the air resistance, and the kinetic energy that is dissipated in braking.

For hydride-powered vehicles with $E/T = 1/3$, equations 2A indicate that the range and speed will be approximately equal to half the magnitudes of ε and ϕ of the hydride.

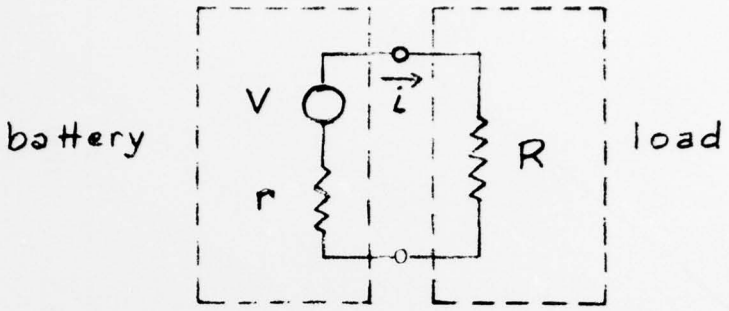

Fig. A1 Model of Battery and Load

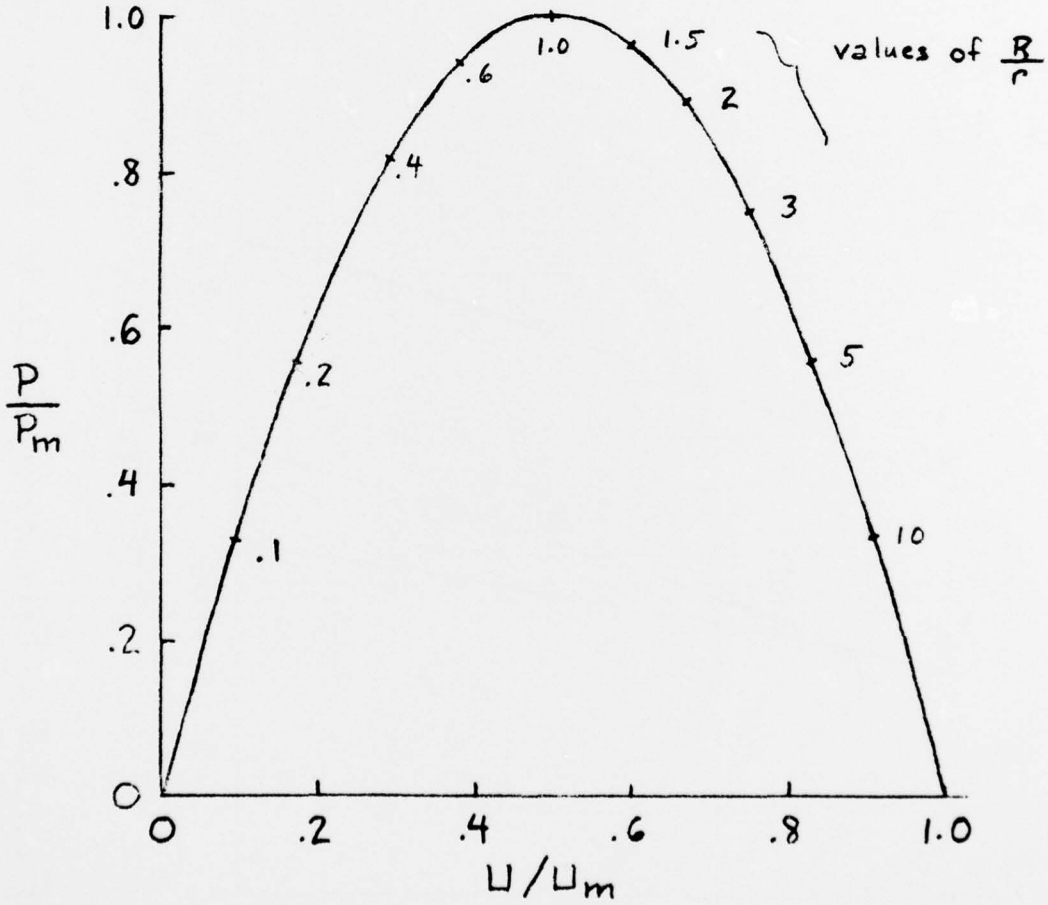

Fig. A2 Ideal Power-Energy Relation for Battery

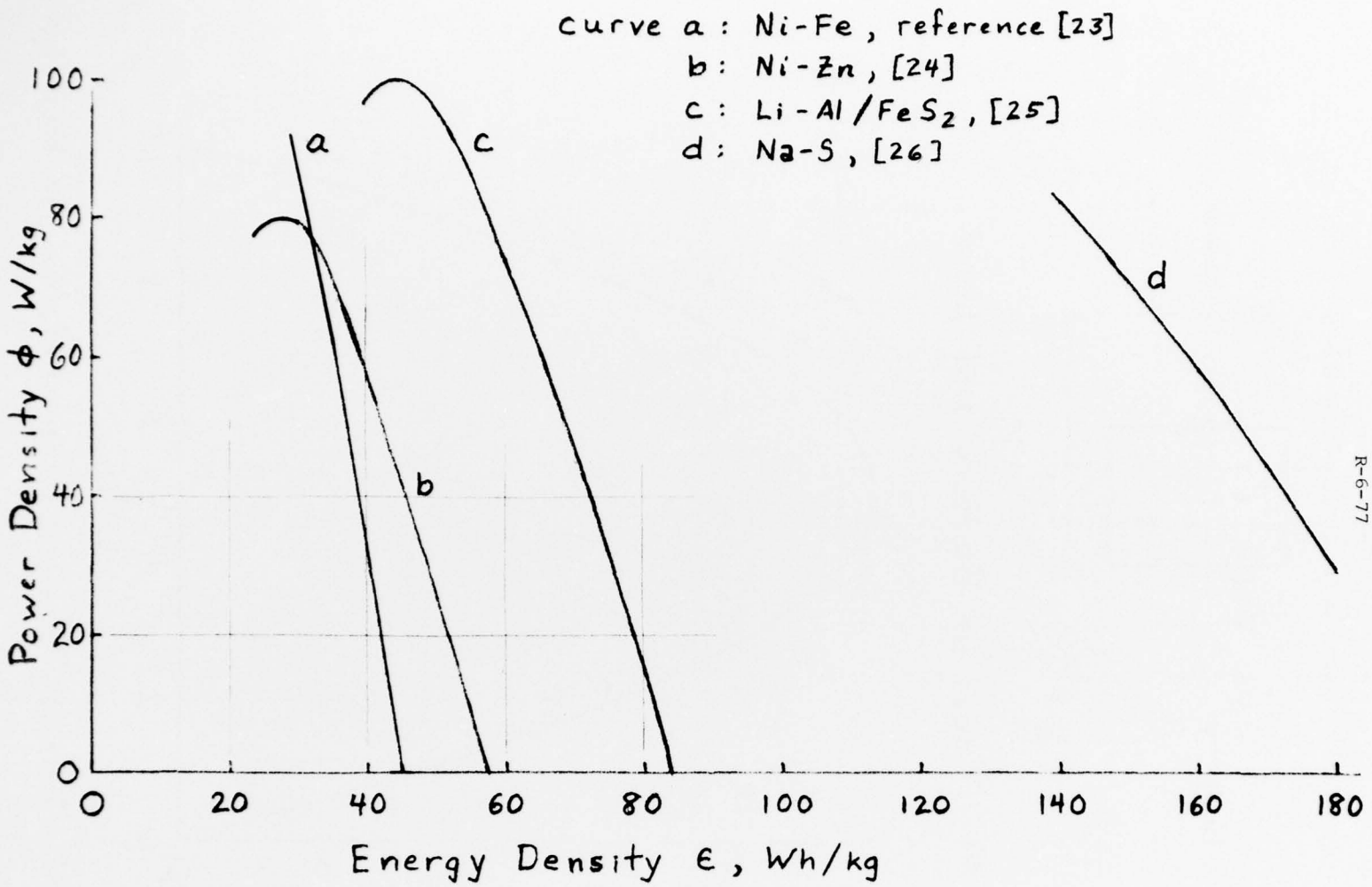

Fig. A3 Performance Data for Various Batteries

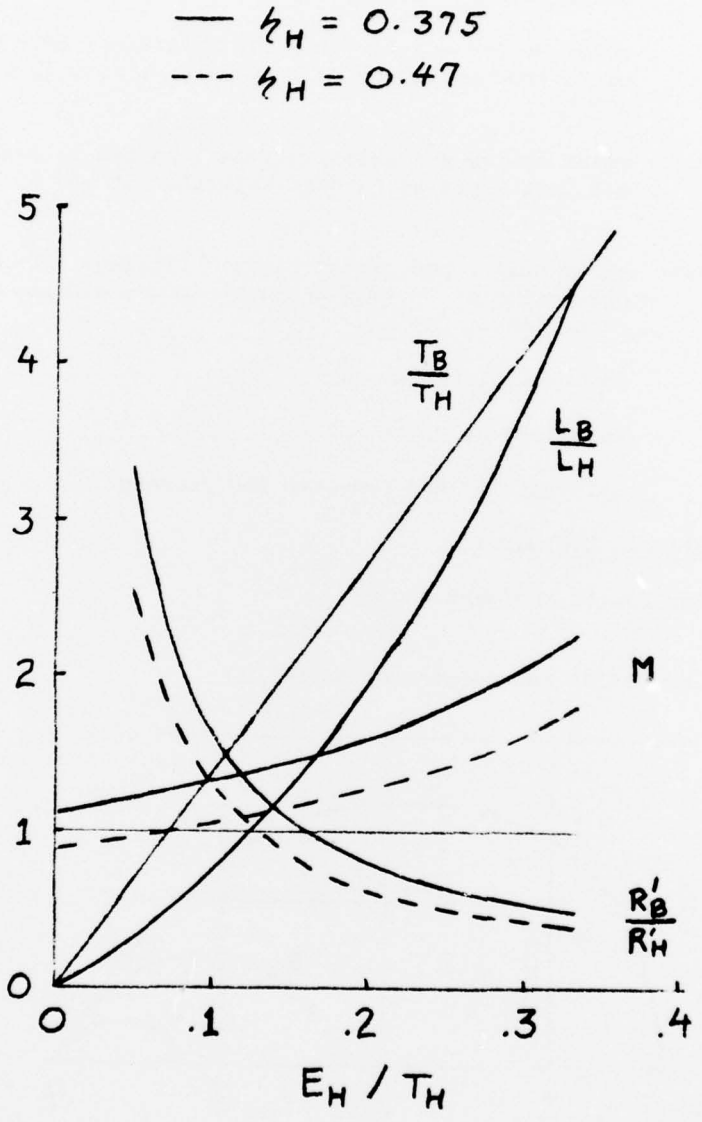

Fig. A4 Comparative Vehicle Performance for Fixed Stored Energy

Theoretical Maxima

solar boiler and heat engine; heat rejection at 300 K

curve 1: solar boiler and direct water splitting; 100% conversion of H_2 free energy to process work, heat rejection at 300 K

solar boiler and water splitting in two or more steps; all heat input at T, heat rejection at 300 K

curves 2&3: solar boiler and direct water splitting; 55% and 30% conversion of H_2 free energy to process work, heat rejection at 300 K

level 4: photovoltaic solar cell

level 5: antenna-type solar cell

point*: solar boiler and two-step ZnO process

More Realistic Estimates

⊙ solar boiler and heat engine

▯ solar boiler and multi-step splitting

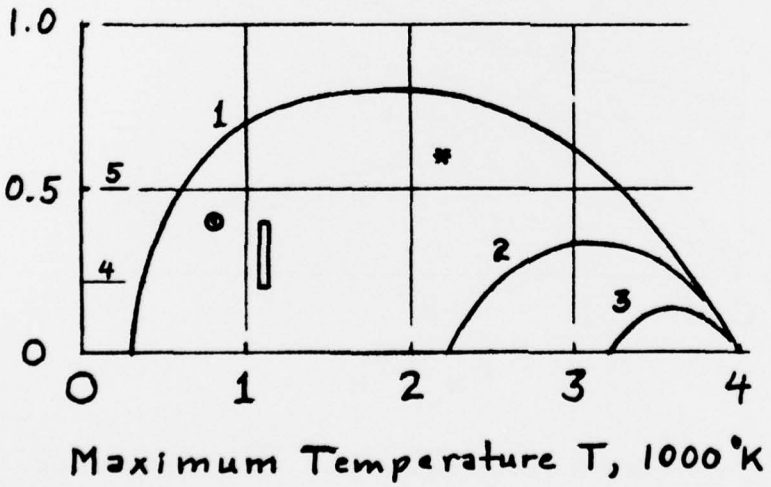

Fig. 1. Thermal Efficiencies for Various Solar Energy Conversion Processes

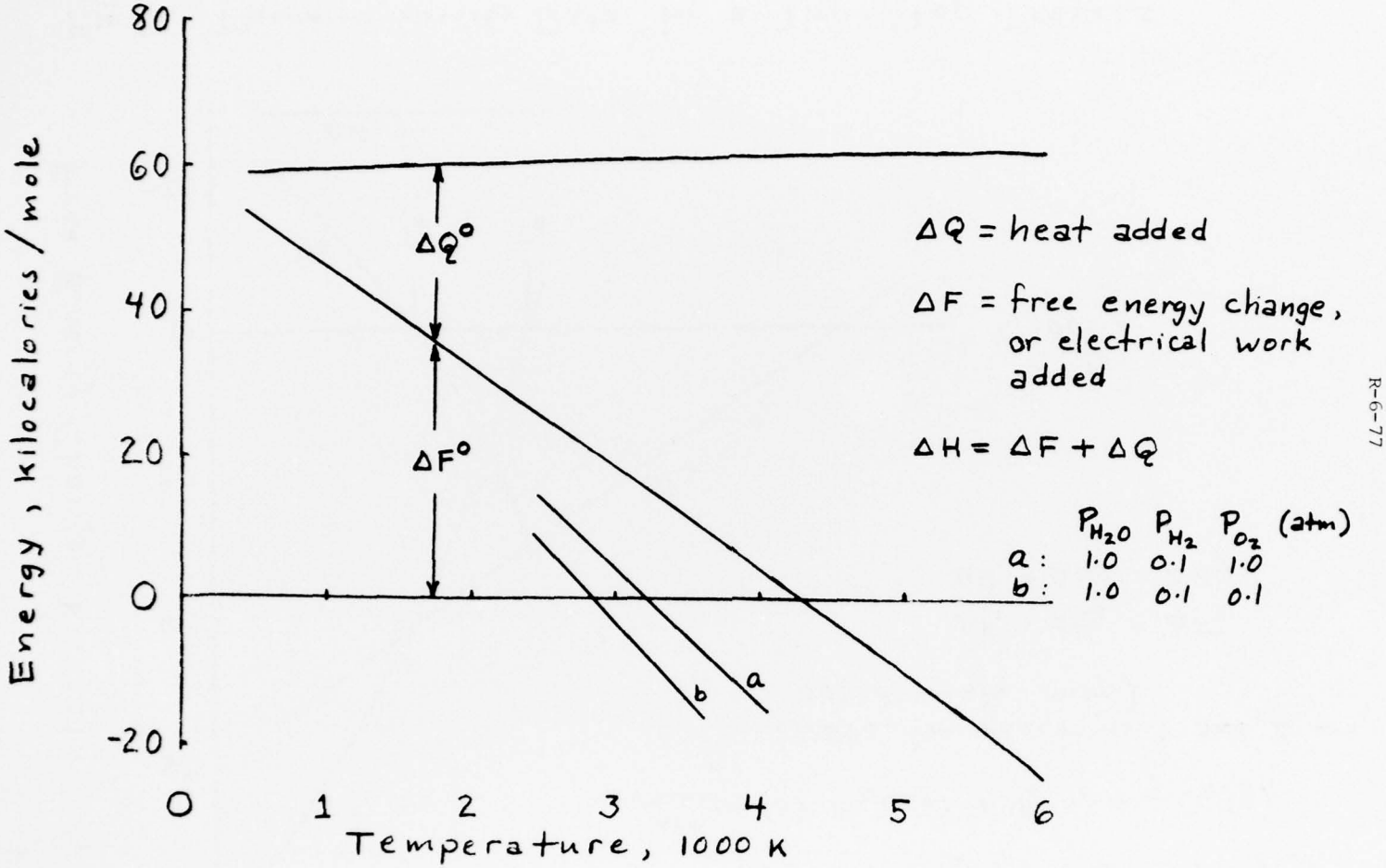

Fig. 2 Thermodynamic Functions for $H_2O(g) \rightarrow H_2(g) + \frac{1}{2} O_2(g)$
Reference: Nat. Bureau Stds., NFRDS - NBS 37, June 1971

R-6-77

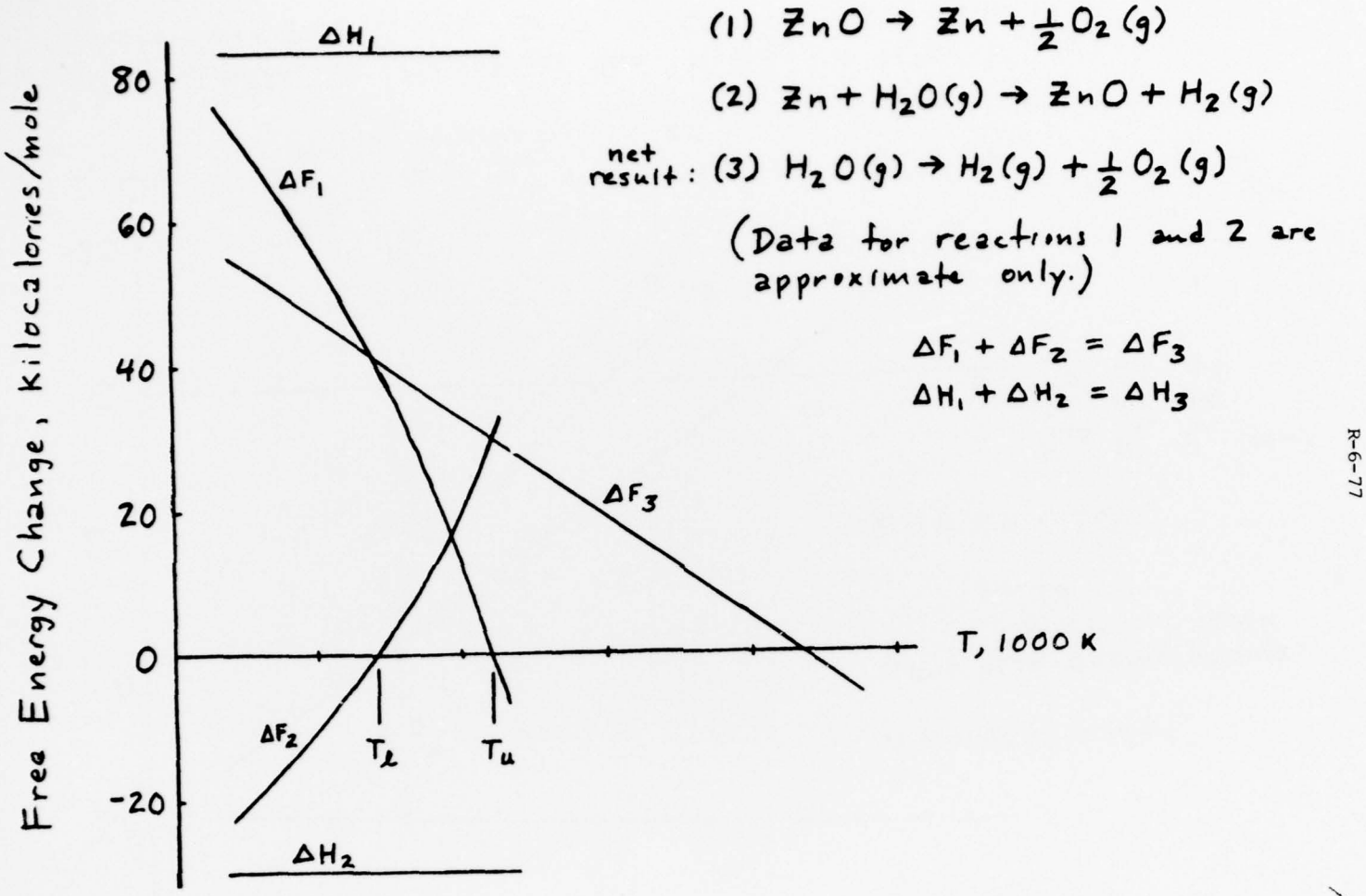

Fig. 3 Thermodynamic Data for a Two-Step Process

(References for ZnO data: Handbook of Chemistry & Physics, 46th ed., p. D-49
ESN 31 July 1976, P. 315)

R-6-77

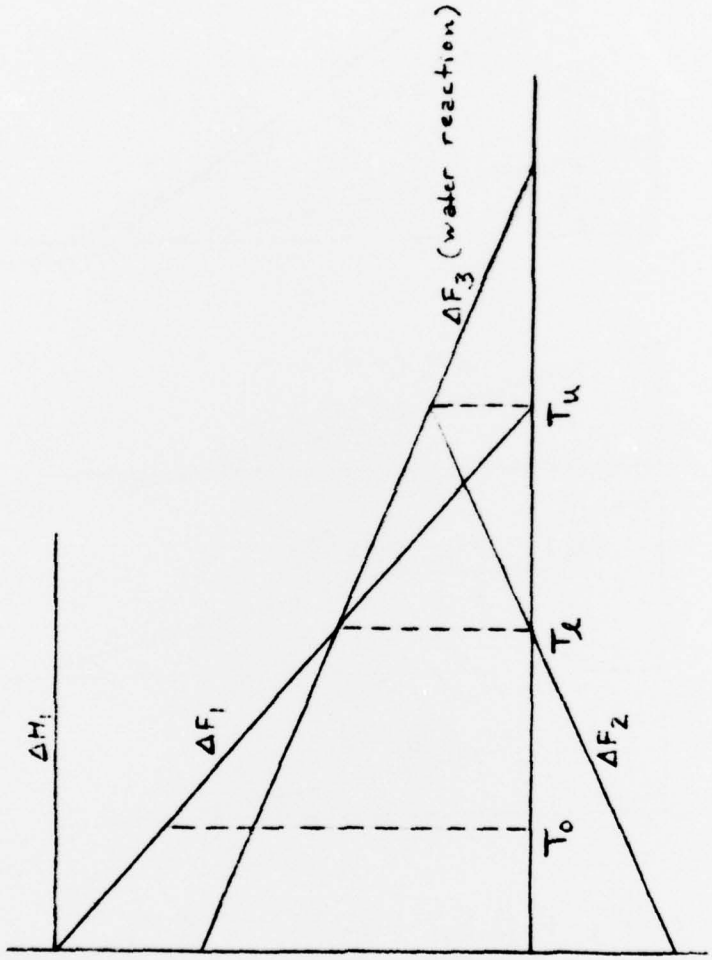

Fig. 4 Straight-Line Model for Two-Step Process

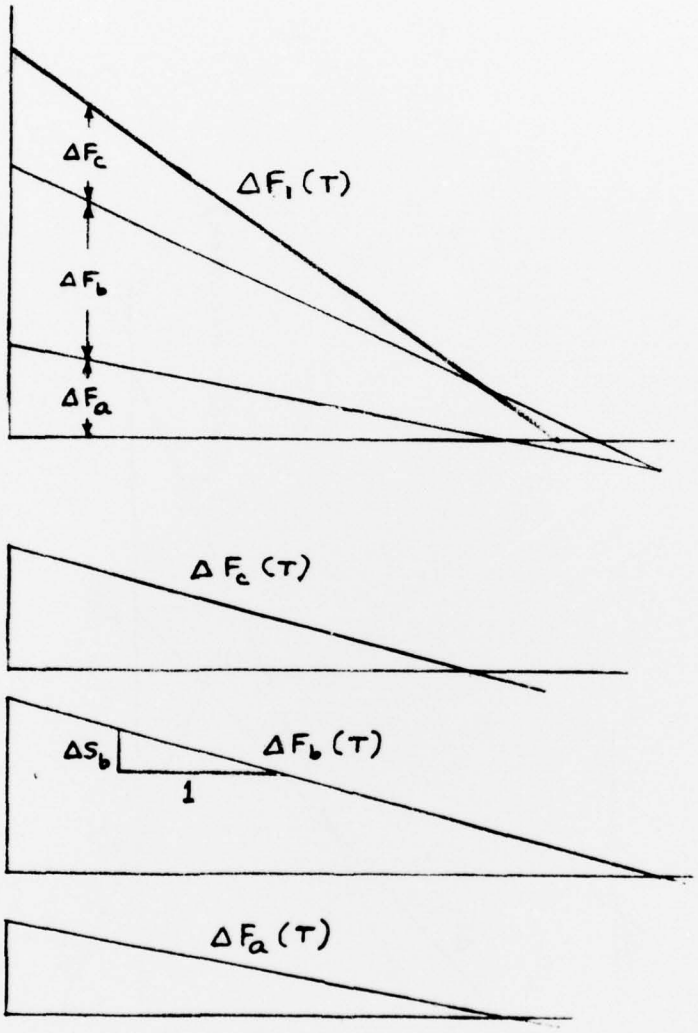

$$\Delta F_a + \Delta F_b + \Delta F_c = \Delta F_1$$
$$\Delta S_a + \Delta S_b + \Delta S_c = \Delta S_1$$

Fig. 5 Net Endothermic Reaction as a Sum of Three Reactions of Smaller Slope ΔS